

## Tilted sandpiles, interface depinning, and earthquake models

A. Malthe-Sørenssen

*Department of Physics, University of Oslo, Box 1048 Blindern, N-0316 Oslo, Norway*

(Received 9 June 1998)

A model of a slowly tilted one-dimensional sandpile with dynamically varying critical slopes is studied. The energy dissipation events are found to be power-law distributed with exponent  $\tau = 1.11 \pm 0.02$  and obey finite size scaling. The model represents a different universality class than the corresponding point driven models. However, the finite size scaling exponent  $D$  and the surface roughness exponent are the same for both driving conditions. The pile height exhibits periodic oscillations, but the oscillation period measured in tilt events diverges as system size increases because the average tilt increment between avalanches is inversely proportional to system size. We demonstrate that the model can be mapped onto a slowly driven interface depinning model and a one-dimensional spring-block model with dynamically varying friction thresholds, supporting a broad universality relating different models of self-organized critical phenomena. [S1063-651X(99)12802-2]

PACS number(s): 64.60.Ht, 05.40.-a, 05.70.Ln

### I. INTRODUCTION

Slowly driven granular systems, such as slowly tilted piles of sand, have served as useful examples to illustrate how some slowly driven dissipative systems evolve into a stationary state characterized by power-law fluctuations in the state variables. The self-tuning of the system to a critical state was termed self-organized criticality (SOC) [1,2], and models based on similar ideas have been used to describe power-law fluctuations in phenomena such as earthquakes [3], evolution [4], and interface growth [5]. Recently, a direct mapping between models of different physical phenomena has demonstrated a broad universality relating sandpile models, interface depinning models, and earthquake train models [6,7] provided specific boundary and driving conditions were applied. It is important to develop similar correspondences also for other models and driving conditions in order to understand the connection between self-organized critical behavior in different systems. In this article we study a simple model of a slowly tilted sandpile and show that the behavior is equivalent to the behavior in uniformly driven interface depinning models [8] and one-dimensional Burridge-Knopoff [9] earthquake models with dynamically varying static friction coefficients.

One of the first experiments to study the applicability of SOC to granular systems was performed by slowly rotating a semicylinder half filled with grains [10]. The distribution of grains flowing out of the system clearly did not support a power-law interpretation, and the system was characterized by a periodic cycling between two angles, which was interpreted as inconsistent with the hypothesis of SOC. The experiments, however, did not address the potential energy of the system, which is the quantity expected to display power-law fluctuations. The internal dynamics were first measured with sufficient resolution for piles of rice [11]. Self-organized critical behavior was observed for long-grained rice, but a characteristic avalanche size appeared for rounder rice, indicating that SOC may be relevant for the description of granular systems, but it is not the universal behavior.

Several features of the rice pile experiments, such as the distribution of transit times [12] and the surface roughness

[13], were well described by the Oslo model sandpile [12]. However, the model did not reproduce the exponent of the avalanche distribution. In the Oslo model the pile is represented by a sequence of columns. If the local slope exceeds a critical value that depends on the local packing configuration, the column topples. The grain is transferred to the next column and a new, random value of the critical slope is chosen, representing a new local packing configuration. The Oslo model can be directly extended to study a slowly tilted system. It is not an entirely realistic model of a tilted granular pile, since in a real pile also the orientations of the grains and therefore the packing stabilities change when the pile is tilted. However, such a model is interesting from a theoretical point of view, because a change in driving conditions is expected to change the scaling behavior of the model.

Tilted granular piles have been studied extensively both experimentally and theoretically. In addition to the experiment by Jaeger *et al.* [10], similar results were found by Bretz *et al.* [14] by tilting a box of grains. The transition to avalanche behavior with rotation speed has also been addressed [15]. However, no systematic experimental studies of the internal avalanches have been performed to establish or contradict a scaling behavior. Theoretical studies have been made based on a continuum description [16,17], on grain simulations [18], and on cellular models [19]. The observed behavior depended on the modeling approach, but the applicability of the models cannot be evaluated without a comparable experimental study.

We have applied the Oslo model to study a slowly tilted pile of grains. The Oslo model has an indirect experimental basis because it reproduces features of slowly driven piles of rice. The tilted sandpile model produces power-law distributed energy dissipation events with an exponent  $\tau = 1.11 \pm 0.02$ . This indicates that the model is in a different universality class than the point driven Oslo model. However, the scaling of the active zone and the finite size scaling exponent are the same for both models. The height of the pile displays periodic fluctuations with a constant period of one measured in the total tilt of the pile, but the period increases linearly with system size when measured in units of tilt events. We show that the model can be mapped onto a uniformly driven

interface depinning model and a one-dimensional earthquake model with dynamically varying frictional thresholds, thereby confirming a broad universality between these self-organized critical phenomena.

## II. TILTED SANDPILE MODEL

The tilted sandpile model is defined in terms of the local slopes of the pile surface,  $z_i$ , at positions  $i$  ranging from the top of the pile at  $i=1$  to the outlet at  $i=L+1$ . The height of the pile at a position  $i$  is given by the sum of local slopes. A column becomes unstable and topples if the local slope exceeds a critical value  $z_i^c$ . During toppling, a new value for  $z_i^c$  is chosen, and a grain is transferred down the pile, resulting in a redistribution of slopes:  $z_i \rightarrow z_i - 2$ ,  $z_{i\pm 1} \rightarrow z_{i\pm 1} + 1$ . Grains that move out of the pile (to position  $i=L+1$ ) are removed. All unstable neighbors are also toppled, and the process is repeated until all sites are stable. The toppling dynamics is identical to the Oslo model sandpile [12], however, the driving conditions are different for the tilted model. A slow tilting is implemented by a gradual, uniform increase of all slopes until a site becomes unstable and topples. All subsequent topplings are resolved before the system is tilted again, ensuring that the pile is infinitely slowly driven. The values of the critical slopes are real numbers chosen randomly between 1 and 2. A change in the range of the critical slopes only implies a rescaling of the vertical axis and does not produce a significant change in behavior.

The avalanche behavior of the system is characterized by the energy dissipation  $E$ , the number of grains leaving the system,  $D$ , called the drop number, and the duration of the avalanches measured as the number of generations of toppling events,  $T$ . The temporal development of the system is characterized by the slope increments  $\delta z$ , between each avalanche. The system has two time scales, the time  $t$ , measured in the number of tilt events, and the total tilt  $Z(t)$ ,

$$Z(t) = \sum_{i=1}^t \delta z_i. \quad (1)$$

The spatiotemporal development of the pile is studied through the time development of the height field  $h_i(t)$  as a function of both time  $t$ , and total tilt  $Z(t)$ .

Figure 1(a) shows a plot of  $P(E,L)$ , the probability density for energy dissipation events  $E$  in a system of size  $L$ . The distribution is consistent with a power law with a finite size cutoff that increases systematically with  $L$ . The finite size scaling plot in Fig. 1(b) shows that the density can be written on a scaling form

$$P(E,L) = L^{-\beta} f(EL^{-\nu}), \quad (2)$$

where  $f(x)$  is a power law  $x^{-\tau}$  for  $x < x_0$  and a cutoff function for  $x > x_0$ . The best data collapse was found for  $\beta = 2.5 \pm 0.03$  and  $\nu = 2.25 \pm 0.03$ . For the largest system size, the power-law exponent was found to be  $\tau = 1.10 \pm 0.03$ . The finite size scaling exponents and the power-law exponent are related through scaling relations. The normalization of the probability density implies that  $\beta > \nu$  and that  $\tau = \beta/\nu$ . The finite size scaling collapse therefore implies that the power-law exponent is  $\tau = 1.11 \pm 0.02$ , which is consistent with the

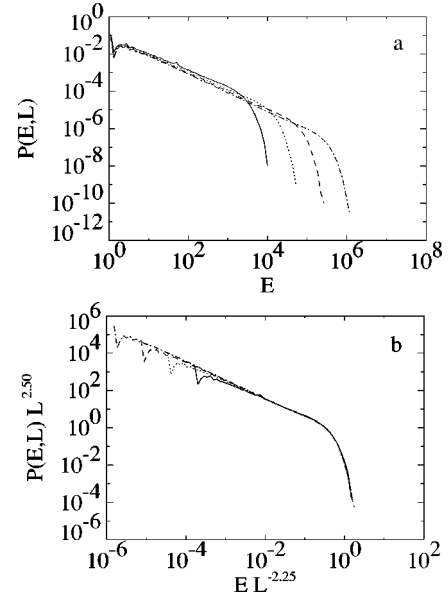


FIG. 1. A plot of the probability density  $P(E,L)$  for an energy dissipation event  $E$  in a system of size  $L$ . (a) shows a direct plot for  $L=50, 100, 200$ , and  $400$ . (b) shows a finite size scaling data collapse on the form  $P(E,L) = L^{-\beta} f(EL^{-\nu})$ .

value found by direct measurement. Another scaling relation can be found from the average energy dissipation [20]. For a pile tilted at an angle  $\delta z \ll z$ , where  $z$  is the slope of the pile, the energy increase is proportional to  $\delta z L^3$ . In a stationary state, the average energy increment must equal the average dissipated energy,  $\langle E \rangle \propto \langle \delta z \rangle L^3$ . The average slope increments can be calculated exactly if we assume that  $z_i^c - z_i$  are independent random variables with a uniform distribution (see, for example, Ref. [21] for details) giving  $\langle \delta z \rangle \propto L^{-1}$ . We expect a similar behavior for the tilted pile and show further on that this is indeed observed for the simulated pile. The average dissipated energy can also be calculated from the scaling form of  $P(E,L)$ :  $\langle E \rangle \propto L^{2\nu - \beta}$ . The stationarity of the pile therefore implies that  $2\nu - \beta = 2$ . This is consistent with the results found for the data collapse. The power-law exponent can be found directly from  $\nu$ :

$$\tau = \frac{2\nu - 2}{\nu} = 1.11 \pm 0.02. \quad (3)$$

Figure 2 shows a finite size scaling plot of the distribution of drop events,  $P(D,L)$ , for different system sizes. The ex-

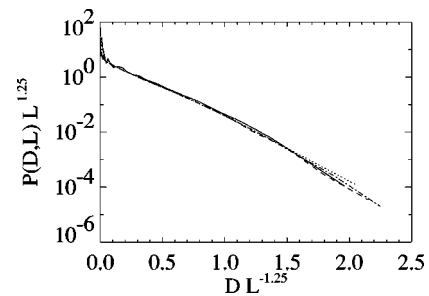


FIG. 2. A scaling data collapse plot of the probability density  $P(D,L)$  for a drop event of size  $D$  in a system of size  $L$  for  $L=50, 100, 200$ , and  $400$ .

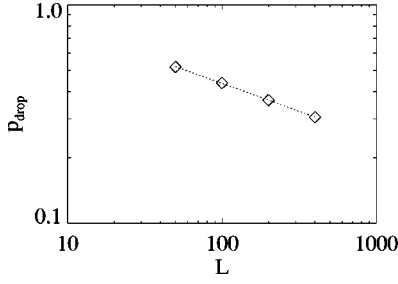


FIG. 3. A plot of the probability of a drop event,  $p_{\text{drop}}$ , as a function of system size  $L$ . The behavior is consistent with a power law with exponent  $\xi_D = 0.25 \pm 0.05$  as illustrated with the dotted line.

ponents that produced the best data collapse were  $\beta_D = 1.25 \pm 0.03$  and  $\nu_D = 1.25 \pm 0.03$ . The distribution is approximately consistent with an exponential distribution. The finite size scaling exponent  $\nu_D$  is related to the exponent for the energy dissipation events,  $\nu_D = \nu - 1$ , as expected from simulations of similar models [20]. It is important to realize that  $P(D, L)$  is a conditional probability density and represents the probability of a drop of size  $D$  given that a drop occurs. The probability of the drop event is a decreasing function of  $L$ . Figure 3 shows that the probability of a drop event  $p_{\text{drop}}$  decreases as a power law with system size  $p_{\text{drop}} \propto L^{-\xi_D}$ , where  $\xi_D = 0.25 \pm 0.05$ .

The avalanches were also characterized by the duration of avalanches, measured as the number of toppling cycles,  $T$ . This is, however, an artificial time scale, since the relaxation dynamics does not include a coupling to a physical time scale through Newton's equations. The distribution of avalanche durations is shown in Fig. 4. The distribution function satisfies the scaling form presented above, with finite size scaling exponents  $\beta_T = 1.70 \pm 0.05$  and  $\nu_T = 1.45 \pm 0.05$ . The power-law exponent was estimated from the largest system size to be  $\tau_T = 1.15 \pm 0.1$ , which is also consistent with the measured value of  $\beta_T$  and  $\nu_T$ :  $\tau_T = \beta_T / \nu_T = 1.20 \pm 0.05$ .

The pile is tilted in small increments,  $\delta z$ . We have argued that the average value of  $\delta z$  is inversely proportional to the system size  $L$ . Figure 5 shows a scaling collapse plot of the probability density  $P(\delta z, L)$  for a slope increment  $\delta z$  in a system of size  $L$ . The scaling collapse indicates that the density is on the form

$$P(\delta z, L) = L^{-\beta_z} f_z(\delta z L^{-\nu_z}), \quad (4)$$

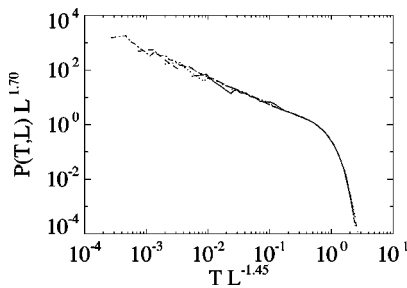


FIG. 4. A plot of the probability distribution  $P(T, L)$  for an avalanche duration  $T$  in a system of size  $L$  for  $L = 50, 100, 200$ , and  $400$ .

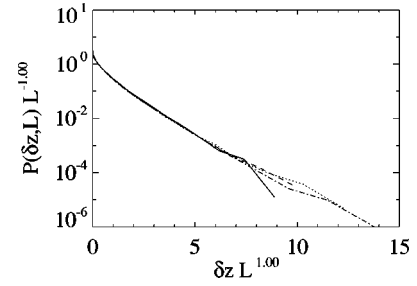


FIG. 5. A finite size scaling plot of the probability density  $P(\delta z, L)$  for the slope increment to be  $\delta z$  between two successive avalanches in a system of size  $L$  for  $L = 50, 100, 200$ , and  $400$ .

where  $f_z(x)$  is approximately an exponential function, and the best data collapse is obtained for  $\beta_z = \nu_z = -1.0 \pm 0.1$ , which implies that  $\langle \delta z \rangle \propto L^{\nu_z}$ , consistent with the predictions above. Since the average slope increment decreases with system size, the two time scales  $t$  and  $Z(t)$  also change relative to each other when the system size is increased. The number of time steps,  $t$ , needed to increase the slope by one is proportional to the system size  $L$ .

The dynamical evolution of the pile is characterized by the temporal development of height of the profile,  $h(x, t, L)$ , as shown in Fig. 6 for  $x = L/2$ . The height  $h(x = L/2, t, L)$  is an intermittent signal with a variety of small and large changes. However, the variation of the curve is restricted by a length scale that depends on the system size. This dependence is characterized by the two-point time correlation function

$$C_2(\tau, x, L) = \langle [h(x, t + \tau, L) - h(x, t, L)]^2 \rangle_t. \quad (5)$$

Figure 7 shows a scaling collapse plot of  $C_2(\tau, L/2, L)$  for different system sizes on the form

$$C_2(\tau, L/2, L) = L^{\beta_h} f_h(\tau L^{-\nu_h}). \quad (6)$$

The correlation function crosses over from an increasing function for  $\tau < \tau_h$  to a constant value for  $\tau > \tau_h$ . For larger  $\tau$ , periodic oscillations of the height change the behavior of the correlation function, but a reasonable data collapse was obtained for small  $\tau$ . The crossover time is a power of the system size,  $\tau_h \propto L^{\nu_h}$ , with  $\nu_h = 0.25 \pm 0.05$ . The width of the active zone during avalanches is given by the standard deviation of the height,  $\sigma_h^2 \propto C_2(\infty, L/2, L) \propto L^{\beta_h}$ . The front width therefore scales with exponent  $\chi = \beta_h/2 = 0.25 \pm 0.03$ , which is the same as for the point driven Oslo model.

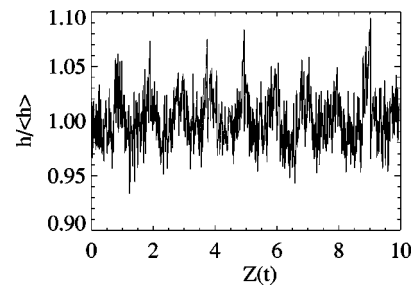


FIG. 6. A plot of the height  $h(x = L/2, L)$  at position  $x = L/2$  in a pile of size  $L = 100$ .

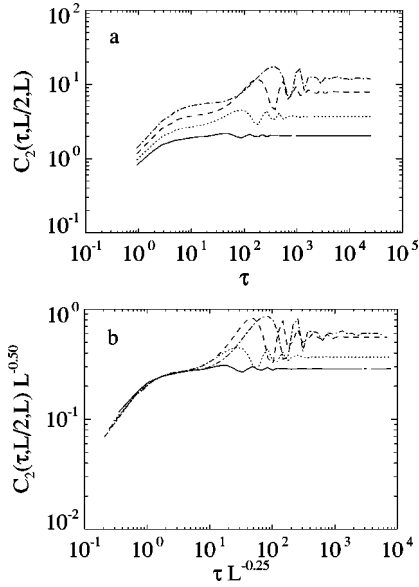


FIG. 7. A plot of the time correlation function  $C_2(\tau, L/2, L)$  for the height of the pile at position  $x = L/2$  for piles of size  $L = 50, 100, 200,$  and  $400$ . (a) shows the direct plot and (b) a finite size scaling data collapse. The collapse is satisfactory for small  $\tau$  and displays a crossover from an increasing function to a constant at  $\tau_h$ . However, for large  $\tau$  a periodic behavior is clearly evident and the finite size scaling breaks down.

A closer examination of the variation of  $h(L/2, t, L)$  shows that the behavior is periodic in time. The periodic behavior is clearer if time is measured in total tilt  $Z(t)$ . The power spectrum  $S(f)$  shown in Fig. 8 shows a distinct peak for  $f = 1.00 \pm 0.01$ , which corresponds to a period  $Z = 1$  in units of slope. The period does not change with system size  $L$ . A similar behavior is observed for the power spectrum for the signal measured with  $t$  as the time unit, but the peak in the spectrum is smeared out. Since the periodicity occurs with a constant period  $Z = 1$ , the average period in units of time  $t$  is  $T = Z / \langle \delta z \rangle \propto L$ . The period is proportional to the system size when measured in units of tilt events. The two time scales therefore reveal a very different behavior in the thermodynamic limit  $L \rightarrow \infty$ : Measured in units of tilt events the period diverges, but measured in units of total tilt the period is constant.

### III. INTERFACE DEPINNING

It has recently been argued that the point driven Oslo model sandpile can be mapped onto a driven interface depinning

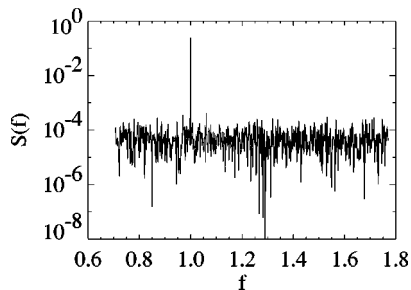


FIG. 8. A plot of the power spectrum  $S(f)$  of the pile height at position  $x = L/2$  for a system of size  $L = 100$ . The spectrum shows a clear peak at  $f = 1.00 \pm 0.01$  indicating a periodicity with period  $z = 1$ . Time is measured in units of slope.

model with quenched disorder which is pulled slowly at one end [6]. Here, we demonstrate that the tilted Oslo model can be mapped onto a uniformly driven interface depinning model. Such a mapping is suggested already by the avalanche exponent  $\tau$  and the avalanche dimension  $D = \nu$  in the tilted model, which are the same as for models of infinitely slowly driven interface depinning [8].

The tilted model is described by the local slopes  $z(x, t)$ , which allows the calculation of the height  $h(x, t)$  as a sum over slopes from the outlet to position  $x$ . The interface depinning model is described in terms of the height  $H(x, t)$  of the interface, which gives the position of the front at a time  $t$ . We apply the mapping of Paczuski and Boettcher [6] and define the height  $H(x, t)$  as the number of topplings in the tilted model in a column at position  $x$ . The local force on the interface is defined to be  $F(x, t) = z(x, t) - z^c(x, t)$ . The dynamically varying critical slopes  $z^c(x, t)$  can be written as a quenched noise  $z^c(x, t) = \eta(x, H)$ , since they are only changed when the column at position  $x$  topples, which corresponds to an increase in  $H$ . The force is increased slowly until it exceeds zero, which results in a depinning and displacement of the interface. The height  $H(x, t)$  can be expressed through the height  $h(x, t)$  of the sandpile,

$$h(x, t) = xZ(t) + H(x-1, t) - H(x, t). \quad (7)$$

The height  $h(x, t)$  at position  $x$  is given by the general tilt of the surface at position  $x$ , which is  $xZ(t)$  if the outlet is at position  $x=0$  and  $Z(t)$  is the cumulative slope increment at time  $t$ , and by the difference between the number of grains toppling into and out of column  $x$ . The local slope can be expressed as a difference in heights,  $z(x, t) = h(x, t) - h(x+1, t)$ , which produces a simplified relation for the local force

$$F(x, t) = -Z(t) + H(x-1, t) - H(x, t) - H(x, t) + H(x+1, t) - \eta(x, H), \quad (8)$$

where the difference in  $H$  is a finite difference formulation of the second derivative

$$F(x, t) = -Z(t) + \nabla^2 H(x, t) - \eta(x, H). \quad (9)$$

This is exactly the form of the uniformly driven interface depinning problem with quenched disorder [8] since  $\eta(x, H)$  is an uncorrelated random function representing quenched noise.

We have therefore demonstrated that the tilted Oslo model can be mapped onto a slowly driven interface depinning model with quenched noise. The mapping is also supported by the exponents characterizing the dynamics. For the tilted Oslo model the avalanche exponent is  $\tau = 1.11 \pm 0.02$ , whereas for the interface depinning model in  $1+1$  dimension it is  $\tau \approx 1.12$  [22]. The finite size scaling exponent  $\nu$  is  $\nu = 2.25 \pm 0.03$  for the Oslo model and  $D = 2.23 \pm 0.03$  for the interface depinning model [6]. This implies that the interface roughness is  $\chi = D - 2$ , which is directly measured in the tilted Oslo model to be  $\chi = 0.25 \pm 0.05$ . Also the distribution of avalanche durations,  $T$ , displayed similar behavior in the two models. For the tilted Oslo model, the cutoff for the avalanche duration scaled with system size with expo-

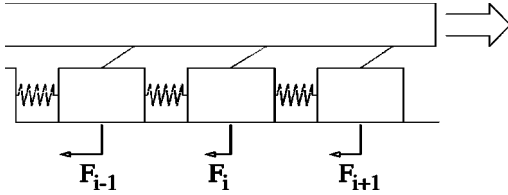


FIG. 9. An illustration of the one-dimensional earthquake model. A set of interconnected blocks rests on a supporting plate and is pulled by springs connected to a slowly driven plate above. The blocks experience static friction forces  $F_i$  to the supporting plate.

ment  $\nu_T = 1.45 \pm 0.05$ , which is in good correspondence with the value  $z \approx 1.42$  found numerically for the constant force depinning transition [22].

#### IV. EARTHQUAKE MODELS

Slowly driven interface depinning models have recently been shown to behave as simple earthquake models with random static friction thresholds [7,23]. Here, we demonstrate that the tilted Oslo model can be mapped onto a similar earthquake model, corresponding to a one-dimensional Olami-Feder-Christensen (OFC) model [3] with random static friction thresholds.

Several theoretical models have been used to address the stick-slip dynamics of tectonic plates in the earth's crust [9,24–26]. The one-dimensional OFC model consists of a sequence of blocks interconnected by springs resting on a supporting plate. The blocks are pulled by weak springs coupled to another plate, representing the slow buildup of stress within or between two surfaces as illustrated in Fig. 9. The blocks are attached to the supporting substrate by static friction forces. When a static friction force exceeds its maximum threshold, the block slides to a position of zero force, increasing the forces on the surrounding blocks. A single displacement can therefore lead to an avalanche of displacements. This corresponds to a one-dimensional version of the OFC model, where the avalanche dynamics is given in terms of the static friction force  $F_i$  on each block. When  $F_i > F_i^c$  an avalanche occurs and the forces are redistributed on the neighboring blocks:  $F_{i\pm 1} \rightarrow F_{i\pm 1} + \alpha F_i$  and  $F_i \rightarrow 0$ . The factor  $\alpha$  is introduced since the redistribution of forces does not have to be conservative. Here, we only address the case where  $\alpha = 1/2$ , which corresponds to the conservative case. When the rightmost (end) block at  $i = L$  is relaxed, all the force is transferred to the neighboring block ( $i = L - 1$ ). The force transferred out of the system at  $i = 1$  is lost. The system is slowly driven: the forces are increased slowly until an avalanche occurs.

The description of the model is almost identical to the description of the Oslo model when the static friction thresholds are chosen to be dynamically varying random variables that are changed after each block displacement. The differences are in the block relaxation, which is to zero force, the boundary conditions at  $i = L$ , and the possible introduction of nonconservative dynamics. The similarity is confirmed by simulations of this system as shown in Fig. 10. The avalanche size is measured as the number of block relaxations, which corresponds to the number of topplings (or the energy

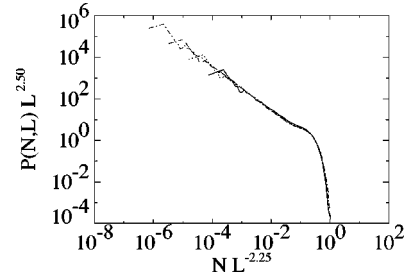


FIG. 10. A plot of the probability distribution  $P(N,L)$  of the number of displacement events,  $N$ , in a one-dimensional earthquake model of size  $L$  for  $L = 50, 100, 200$ , and  $400$ . The best data collapse produced the finite size scaling exponents  $\nu_N = 2.25 \pm 0.02$  and  $\beta_N = 2.50 \pm 0.05$ . The distribution is consistent with a power law with exponent  $\tau = 1.10 \pm 0.05$ .

dissipation) in the tilted Oslo model, and the avalanche exponent and the finite size scaling behavior are the same as for the tilted Oslo model. We conclude that the tilted Oslo model can be mapped onto a one-dimensional earthquake model with dynamically varying static friction thresholds. Simulations of non-conservative versions of the model corresponding to  $\alpha < 1/2$  did not produce a critical behavior. A lower value of  $\alpha$  introduced a characteristic length scale that was reflected in the distribution of avalanche sizes. The model is therefore only critical in the conservative limit,  $\alpha = 1/2$ .

#### V. CONCLUSIONS

We have studied a simple model of a slowly tilted pile of grains based on the Oslo model sandpile. The model displayed power-law distributed energy dissipation events with an exponent  $\tau = 1.11 \pm 0.02$ . Consequently, the tilted Oslo model represents a different universality class than the point driven Oslo model, for which  $\tau = 1.53 \pm 0.02$ . The universality class therefore depends on the external driving. However, the finite size scaling exponent  $\nu$  is the same for both models.

The behavior of the system is characterized by two time scales, the number of tilt events  $t$  and the total tilt  $Z(t)$ . The pile is characterized by periodic fluctuations in the height with a period  $Z = 1$ , but the period measured in tilt events is proportional to  $L$ . Large systems must therefore be driven at a slower rate in order to retain a critical behavior. It is important to consider this relation between physical time, measured by  $Z(t)$ , and the event time  $t$  in experimental studies at finite tilting rates. We observe that the system displays self-organized critical behavior even though periodic oscillations are observed for finite system sizes.

The temporal evolution of the pile was characterized by the time correlation function of the height. The crossover time  $\tau_h$  is interpreted as the time until a large avalanche reaches  $x = L/2$ , and significantly changes the profile. The scaling behavior  $\tau_h \propto L^{\nu_h}$ , with  $\nu_h = 0.25 \pm 0.05$ , is significantly different from the results of the point driven Oslo model, for which  $\nu_h = 1.25 \pm 0.05$ . The difference is due to the different driving conditions. Since the avalanches in the tilted Oslo model are triggered all along the profile, more avalanches reach  $x = L/2$ . However, the surface roughness  $\chi$  is the same for both models.

The tilted sandpile model can be mapped onto an infi-

nitely slowly, uniformly driven interface depinning model. The results from the  $(1+1)$ -dimensional driven interface depinning models can therefore be applied to the tilted sandpile model. This might allow a discussion of the behavior at finite tilting rates without a direct simulation of the tilted model. It would also be interesting to test if a similar mapping also can relate higher-dimensional systems of the Oslo model and the driven interface depinning model. The tilted sandpile model can also be mapped onto a one-dimensional slider-block model of earthquakes with dynamically varying static fric-

tion thresholds. This supports the notion of a broad universality in self-organized critical systems observed by Paczuski and Boettcher [6].

#### ACKNOWLEDGMENTS

I thank Maya Paczuski, Kim Christensen, and Jens Feder for stimulating discussions. The project was supported by NFR, the Norwegian Research Council, through a grant of computer time.

- 
- [1] P. Bak, C. Tang, and K. Wiesenfeld, *Phys. Rev. Lett.* **59**, 381 (1987).
  - [2] P. Bak, C. Tang, and K. Wiesenfeld, *Phys. Rev. A* **38**, 364 (1988).
  - [3] Z. Olami, H. J. S. Feder, and K. Christensen, *Phys. Rev. Lett.* **68**, 1244 (1992).
  - [4] P. Bak and K. Sneppen, *Phys. Rev. Lett.* **71**, 4083 (1993).
  - [5] K. Sneppen, *Phys. Rev. Lett.* **69**, 3539 (1992).
  - [6] M. Paczuski and S. Boettcher, *Phys. Rev. Lett.* **77**, 111 (1996).
  - [7] D. Cule and T. Hwa, *Phys. Rev. Lett.* **77**, 278 (1996).
  - [8] M. Paczuski, P. Maslov, and P. Bak, *Phys. Rev. E* **53**, 414 (1996).
  - [9] R. Burridge and L. Knopoff, *Bull. Seismol. Soc. Am.* **57**, 341 (1967).
  - [10] H. M. Jaeger, C.-h. Liu, and S. R. Nagel, *Phys. Rev. Lett.* **62**, 40 (1989).
  - [11] V. Frette, K. Christensen, A. Malthe-Sørensen, J. Feder, T. Jøssang, and P. Meakin, *Nature (London)* **379**, 49 (1996).
  - [12] K. Christensen, A. Corral, V. Frette, J. Feder, and T. Jøssang, *Phys. Rev. Lett.* **77**, 107 (1996).
  - [13] A. Malthe-Sørensen, K. Christensen, V. Frette, J. Feder, and T. Jøssang, report.
  - [14] M. Bretz, J. B. Cunningham, P. L. Kurczynski, and F. Nori, *Phys. Rev. Lett.* **69**, 2431 (1992).
  - [15] J. Rajchenbach, *Phys. Rev. Lett.* **65**, 2221 (1990).
  - [16] J.-P. Bouchaud, M. E. Cates, J. R. Prakash, and S. F. Edwards, *J. Phys. I* **4**, 1383 (1994).
  - [17] A. Mehta, J. M. Luck, and R. J. Needs, *Phys. Rev. E* **53**, 92 (1996).
  - [18] G. Baumann and D. E. Wolf, *Phys. Rev. E* **54**, R4504 (1996).
  - [19] G. C. Barker and A. Mehta, *Phys. Rev. E* **53**, 5704 (1996).
  - [20] A. Malthe-Sørensen, *Phys. Rev. E* **54**, 2261 (1996).
  - [21] R. H. Larsen and M. L. Marx, *An Introduction to Mathematical Statistics and its Applications* (Prentice-Hall International, London, 1986).
  - [22] H. Leschhorn, *Physica A* **195**, 324 (1993).
  - [23] D. Cule and T. Hwa, *Phys. Rev. B* **57**, 8235 (1998).
  - [24] J. M. Carlson and J. S. Langer, *Phys. Rev. Lett.* **62**, 2632 (1989).
  - [25] J. M. Carlson and J. S. Langer, *Phys. Rev. A* **40**, 6470 (1989).
  - [26] H. Nakanishi, *Phys. Rev. A* **41**, 7086 (1990).